NASA

COMBUSTION GENERATED NOISE IN GAS TURBINE COMBUSTORS

by

W. C. Strahle and B. N. Shivashankara

GEORGIA INSTITUTE OF TECHNOLOGY

prepared for

NATIONAL AERONAUTICS AND SPACE ADMINISTRATION

1. Report No. CR 134843	2. Government Accession No.	3. Recipient's Catalog No.
4. Title and Subtitle COMBUSTION GENERATED NOISE IN GAS TURBINE COMBUSTORS		5. Report Date August 1974
		6. Performing Organization Code
7. Author(s) W. C. Strahle B. N. Shivashankara		8. Performing Organization Report No.
		10. Work Unit No.
9. Performing Organization Name and Address Georgia Institute of Technology Atlanta, Georgia 30332		11. Contract or Grant No. NAS3 - 17861
		13. Type of Report and Period Covered Contractor Report
12. Sponsoring Agency Name and Address National Aeronautics and Space Administration Washington, D. C. 20546		14. Sponsoring Agency Code

15. Supplementary Notes

Technical Officer, Ronald G. Huff, NASA Lewis Research Center

2100 Brookpark Road, Cleveland, Ohio 44135

16. Abstract

Experiments are conducted to determine the noise power and spectra emitted from a gas turbine combustor can exhausting to the atmosphere. In addition, limited hot wire measurements were made of the cold flow turbulence level and spectra within the can. The fuels used were JP-4, acetone and methyl alcohol burning with air at atmospheric pressure. The experimental results show that for a fixed fuel the noise output is dominated by the airflow rate and not the fuel/air ratio. The spectra are dominated by the spectra of the cold flow turbulence spectra which were invariant with airflow rate in these experiments. The effect of fuel type on the noise power output was primarily through the heat of combustion and not the reactivity. A theory of combustion noise based upon the flame radiating to open surroundings is able to reasonably explain the observed results. A thermoacoustic efficiency for noise radiation as high as 3×10^{-5} was observed in this program for JP-4 fuel. Scaling rules are presented for installed configurations.

17. Key Words (Suggested by Author(s)) Combustion noise Can combustors Noise		18. Distribution Statement Unclassified - unlimited	
19. Security Classif. (of this report) Unclassified	20. Security Classif (of this page) Unclassified	21. No. of Pages 40	22. Price*

NASA-C-168 (Rev 6-71)

FORWARD

The facility used in this program was designed by Mr. R. A. Cassanova, Research Engineer, and he gave substantial aid in its construction. Mr. Tai-Chen Cho, Graduate Research Assistant, assisted in experimental work and data reduction.

TABLE OF CONTENTS

SUMMARY

A facility has been constructed for acoustically testing gas turbine combustors. Noise measurements have been made on a single combustor burning JP-4, methanol and acetone with air and exhausting to the atmosphere. The flow variables were air flow and fuel/air ratio. Measurements were made of the noise directionality, spectra and overall power output. Auxillary measurements were made of the turbulence intensity and spectra in cold flow, and Pitot pressure profiles were used to determine the velocity distribution interior to the can. A theory of combustion noise was applied to the configuration.

The measured spectra were found to be virtually invariant with a change in operating variables and fuel type. The noise is broadband with a single peak in the vicinity of 400Hz. The invariance of the combustion noise spectra is believed linked to the observed invariance of the cold flow turbulence spectra, following observations on other programs. The noise power output varied as flow velocity to an exponent of 2.5 and was only weakly dependent upon fuel/air ratio. The fuel type appears to affect the noise power output through the heat of combustion rather than through its reactivity. A theoretical basis for these results has been developed.

A thermoacoustic efficiency (ratio of noise power output to the heat release rate) as high as 3×10^{-5} has been measured for JP-4 fuel. This is the highest value ever reported for hydrocarbon-air flames. A formula, based upon a flame burning in open surroundings, has been developed for the scaling law of acoustic power with combustor operating variables.

1

INTRODUCTION

Core noise has been recognized to be one of the important sources of noise from aircraft turbopropulsion systems, especially in the low exit velocity regime such as found in the case of high by-pass turbofan engines, lifting fan configurations and high shaft power gas turbines. Earlier studies on open turbulent flames (ref. 1) have shown that combustion noise predominates over jet noise even at flow velocities of the order of 200 m/sec. An extension of this study showed that noise augmentation results when the flame is enclosed by a duct (ref. 2). That is, wall reflections of the generated pressure waves change the radiation impedance of a flame so that the sound power radiated is augmented over that which would be radiated in the absence of an enclosure. There is clear evidence in the literature (refs. 3 and 4) to show that the noise emitted to the surroundings by combustor-nozzle configurations depends upon the roughness of combustion in the combustion chamber to an appreciable extent. Therefore, it is evident that a study of noise generated by an actual engine combustor is required for understanding of the core noise problem. In the present work noise generation by a combustor taken out of a gas turbine engine is studied. The combustor is operated at atmospheric pressure and no nozzle is used in order to avoid the velocity and temperature gradients a nozzle would introduce and to have a reasonably well-defined acoustic termination. Such an experiment enables a direct evaluation of the noise generation in the combustor provided the acoustical behavior of the combustor walls is accurately known.

Much of the core noise information which has been generated is subject to wide interpretation because the accustics of the engine enclosure affect the amount of noise actually radiated to the surroundings. Furthermore, the type of noise actually in core noise is open to question. That is, if it is combustion noise, is it direct combustion noise or indirect noise (ref. 5)? This report is concerned with direct combustion noise which is generated in and radiated from a region undergoing turbulent combustion. The "entropy noise" (ref.5) has been purposefully removed by the absence of a terminating nozzle on the can. Theoretical acoustics and the experimental results suggest that the configuration of this experiment may be analyzed as though the flame were burning in the open. In other words the can enclosure acoustics affect the acoustic power radiated in only a minor way. In order to translate the results to an actual engine situation, duct acoustics would have to be applied and at least entropy noise would have to be considered as an additional noise source.

The experiments were conducted with total air flow rate through the combustor varying between 11.3 and 28.2 m^3/min (measured at standard temperature and pressure). The fuels used were JP-4, methanol and acetone. The fuel to total air ratio was varied between 0.0017 and 0.022. The combustor operated at atmospheric temperature and pressure.

EXPERIMENTAL APPARATUS AND RESULTS

Apparatus

The combustor used in this study is shown in figure 1. It is a can-type combustor taken out of a Boeing 502-7D gas turbine engine unit with its air inlet slightly modified to adapt to the present experimental set-up. This gas turbine unit has two such combustors which are supplied with air by a compressor at a pressure of three atmospheres. The design compressor flow rate is 1.6 Kg/s.
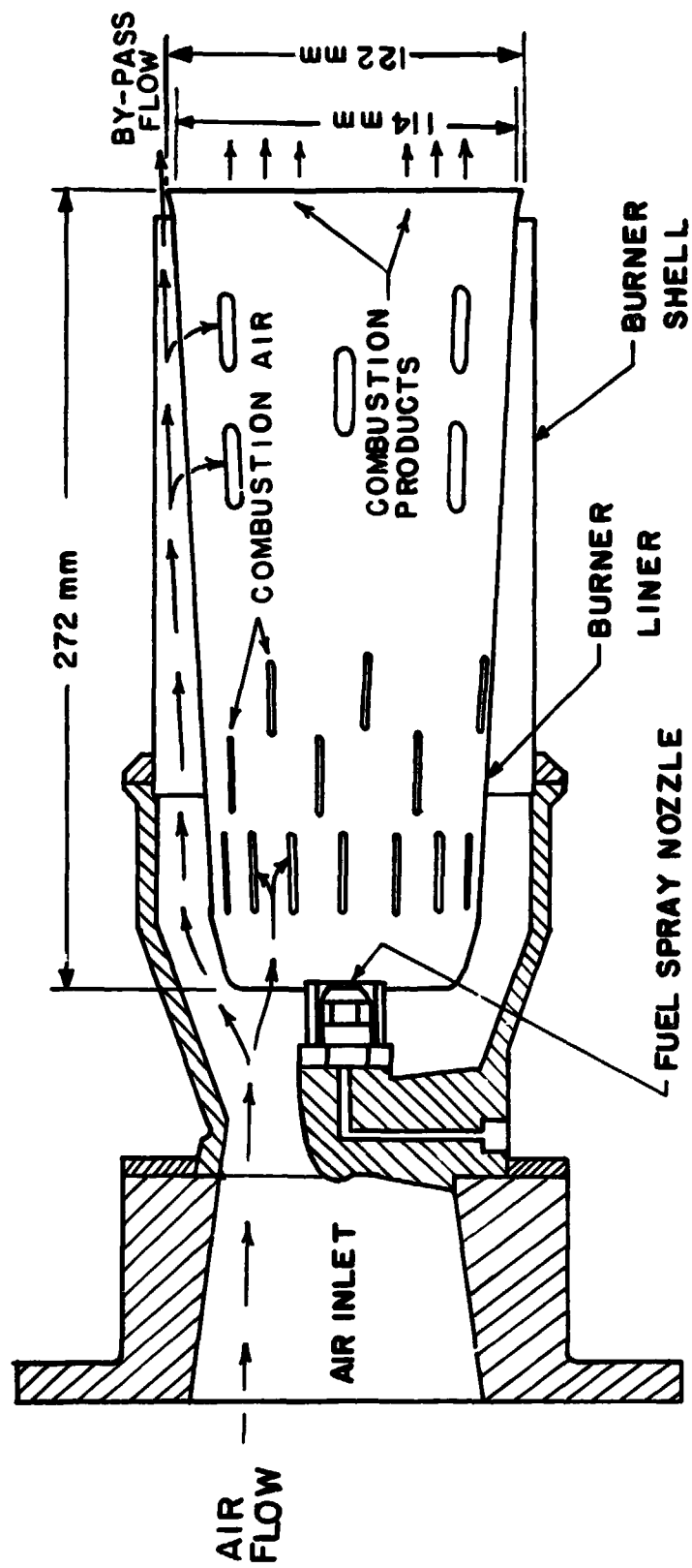
Figure 1. Combustor Details

3

The design fuel consumption rate is 1.1 x 10^{-5} m^3/s at a nozzle operating pressure of 689 kPa. Details may be found in reference 5. Liquid fuel is sprayed inside the burner liner. The liner has slots at both the head end and the walls for air to flow into the combustion region. The rest of the air flow is by-passed between the liner and the burner shell. Ignition of the combustor is achieved by a spark plug. Information on the combustion efficiency or gas temperature range of the burner are not available. However, gas temperature calculations are included later in this report.

The flow system is schematically shown in figure 2. This facility was designed and built during the contract period. Air is supplied from an 861 kPa air reservoir, regulated by a valve and metered by an orifice meter. A muffler is included in the air piping just upstream of the combustor to reduce flow noises. The liquid fuel is fed by gas pressurization. A turbine flow meter is used to measure the flow rate of fuel through the system.

Figure 3 is a photograph of the experimental set-up. The combustor, fuel tank and the air muffler are mounted on a test stand. The test stand is placed on a platform outside the laboratory in such a way that the burner axis is horizontal and at about 2.4 m above the ground level in the forward half-circle. All the flow control valves, flow display units and instrumentation are placed inside the laboratory.

The instrumentation for date acquisition is shown in figure 4(a). Sound pressures are measured by five half-inch condenser microphones mounted on stands and in the same horizontal plane as the burner axis. The microphones are provided with wind shields. Figure 3 shows how the microphones are placed with respect to the combustor. The radius of the microphones in all the experiments is chosen as 3.05 m with the angular locations varying between 15° and 120° to the flow direction. It has been verified that at this distance the sound pressure measurements would correspond to the acoustic far-field. The output from the microphones are read out on a sound level meter. All the five signals are recorded simultaneously on a magnetic tape recorder. Calibration signals are also included on the tape for reference when reproducing data. The data reduction scheme is shown in Figure 4(b). The frequency spectra of noise are obtained using a digital fourier analyzer. The low pass filter is used to prevent the aliasing phenomenon which occurs with digital data.

Flow and Combustion Characteristics

The air entering the combustor was split into two flows. One portion flows through the annulus formed by the inside wall of the outer pipe and the liner and is used to cool the pipe and liner walls before exiting through an annulus located at the end of the combustor. The second part of the flow is used as combustion air and enters the combustion chamber through holes at the inlet and in the liner side walls. In order to determine what percentage of the total air flow is used in the combustion process it is required to experimentally obtain the flow rate of the air through the liner.

Figure 5 shows the details of slot arrangement in the liner. A Pitot tube was traversed inside the liner on stations 1 and 2 in cold flow. Also, a single Pitot pressure measurement was made to determine the velocity of the by-pass air flow. The static pressure was assumed to be the same as the
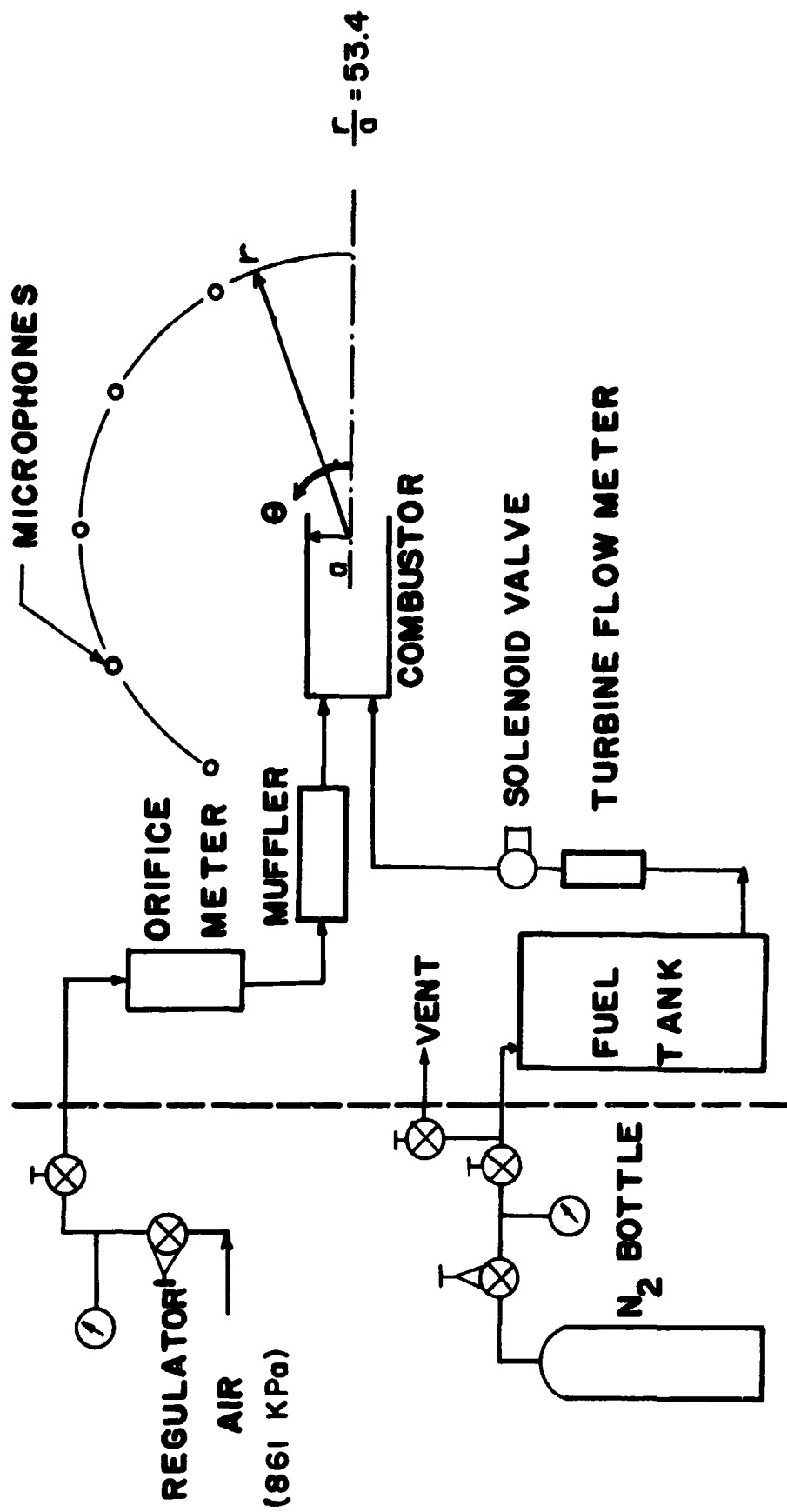
Figure 2. Flow system schematic

MICROPHONES

ORIFICE
METER

MUFFLER

COMBUSTOR

SOLENOID VALVE

TURBINE FLOW METER

VENT

FUEL TANK

REGULATOR

AIR
(861 KPa)

N_2 BOTTLE

$\frac{r}{a} = 53.4$

r

θ
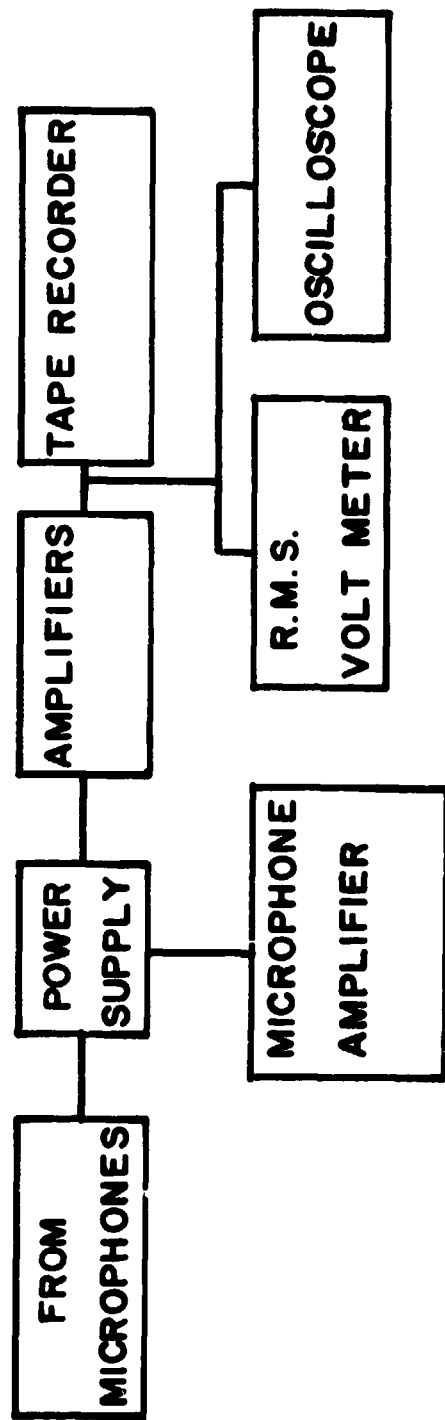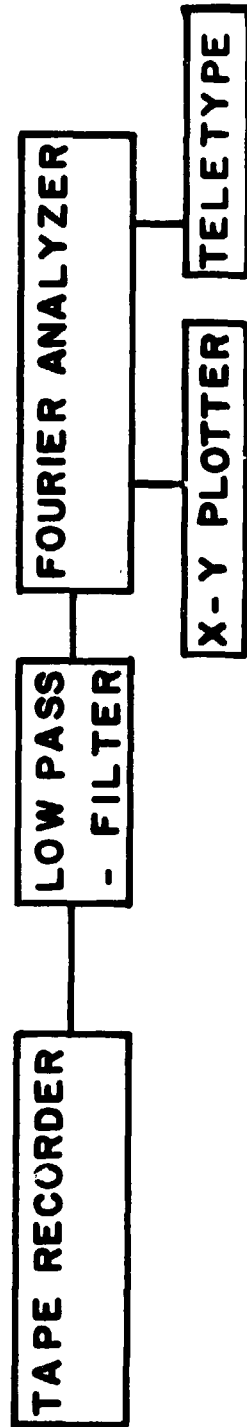
a
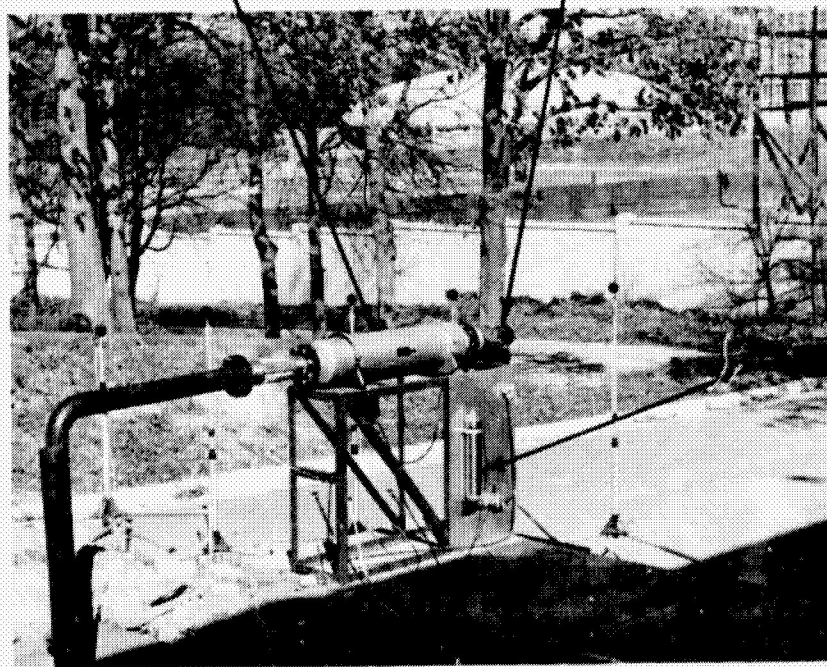
Figure 3. Photograph showing airline muffler, fuel tank and combustor installed on the test stand. The microphones are shown with wind shields installed.

a. DATA ACQUISITION

b. FREQUENCY ANALYSIS
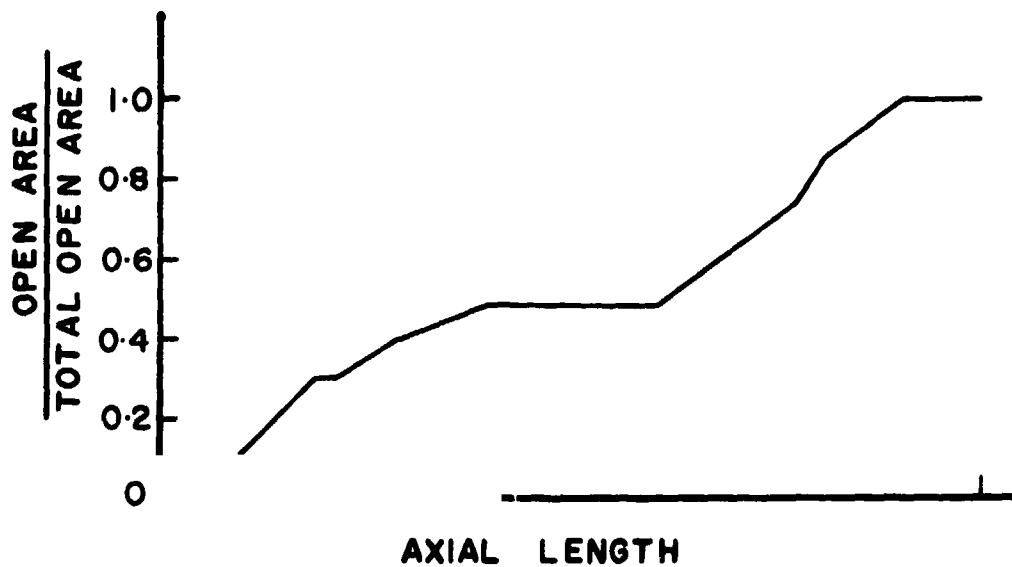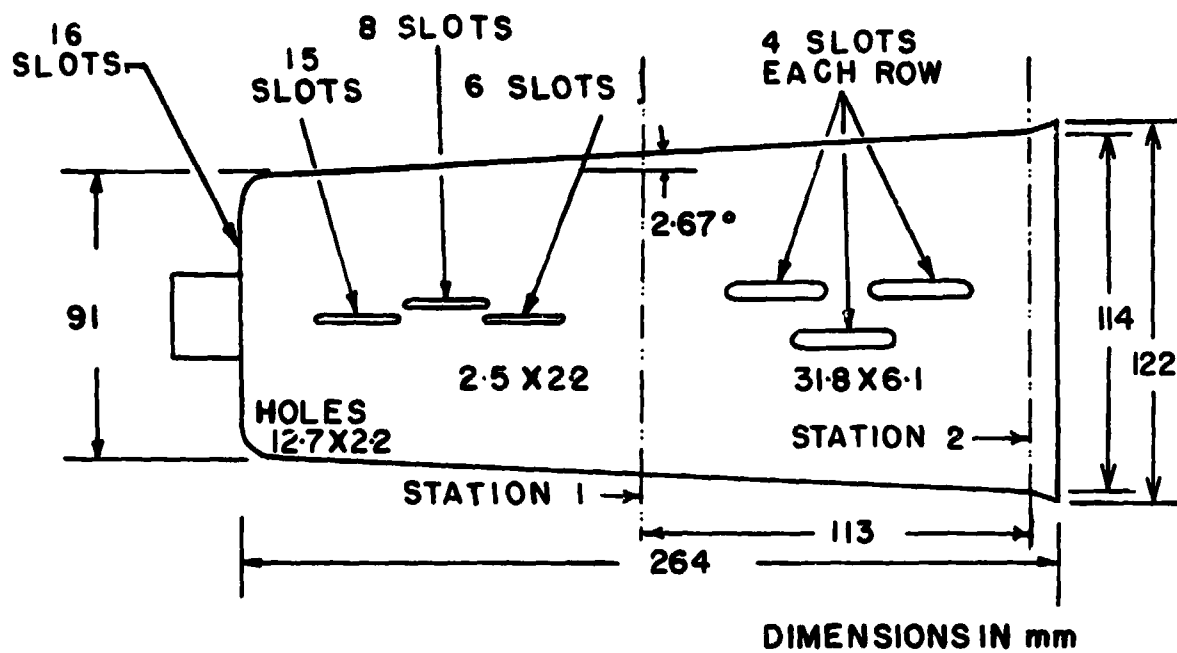
Figure 4. Instrumentation schematic

7

Figure 5. Burner details and slot area distribution
Total open area due to all slots is equal
to 4176 mm^2.

atmospheric pressure. The tube diameter was half of the annulus gap width.

Pitot pressures measured at various flow rates at station 1 showed that up to approximately 25 mm from the liner walls recirculating flow was present which resulted in negative Pitot pressures. Considering that the diameter at this section is only 99 mm the region of recirculating flow is quite appreciable. Therefore, it was not possible to calculate reasonable values for the volumetric flow rate through this section using the Pitot pressure measurements. This problem was compounded because of inaccurate knowledge of the flow directions in this complex flow field. In station 2 the recirculating zone occured up to approximately 10 mm from the walls. The Pitot pressure traverse for station 2 is shown in Figure 6. This also shows the magnitude of the asymmetry of the flow. The liner diameter at this station being 108 mm, the volume flow rate was calculated neglecting the recirculation region and using only the positive Pitot pressure values. This will give a slight overestimate for the air flow through the liner. It was found that over a total air flow rate range from 11.3 to 19.8 m^3/min (at standard temperature and pressure) the air flow into the liner varied between 40-43% of total flow rate. Measurements of the by-pass air velocity with and without combustion showed that the by-pass ratio varied only about 5% from cold flow value. Thus it appears to be adequate to consider that 40% of the total air flows through the liner.

The limits of stable operation for the combustor were determined so that a test matrix for noise measurements could be selected. The blow-out limits were established by setting the fuel flow rate and varying the air flow rate until the flame visibly blew-out. From these data the blow-off curve for JP-4 fuel shown in Figure 7 was plotted. It is seen that the blow-off air flow rate is maximum at a mixture ratio of 0.008 and drops off on either side of this value. The air flow rates and mixture ratios for noise measurement tests were chosen so that stable combustion could be obtained. A detailed blow-off plot was not obtained for acetone and methyl alcohol fuels.

In order to gain a better feel for orders of magnitude involved with various flow parameters the exhaust temperature is required. It was not measured experimentally but calculated from theoretical aerothermochemistry. The charts of reference 7 were used with ethylene assumed as the fuel. The carbon/hydrogen atom ratio of ethylene (1:2) is close to that of JP-4. Figure 8 shows the theoretical exit plane temperature as a function of the overall fuel/air ratio and the fuel/air ratio inside the can assuming 60% bypass flow. Also shown is the ratio of the exit plane speed of sound to the sea level standard speed of sound in air (332 m/s). Looking at the maximum flow rate point on Figure 7 and using the known geometry of the chamber, the maximum exhaust velocity is roughly 50 m/s and the Mach number is roughly 0.08. The exit plane flow is therefore characterized as a low Mach number flow. One complication in calculating the exit plane speed of the bypass flow is the lip on the can which protrudes into the bypass stream (see figure 1). Since the effective cross-section area is difficult to compute no representative numbers are given for the bypass flow exit velocity.
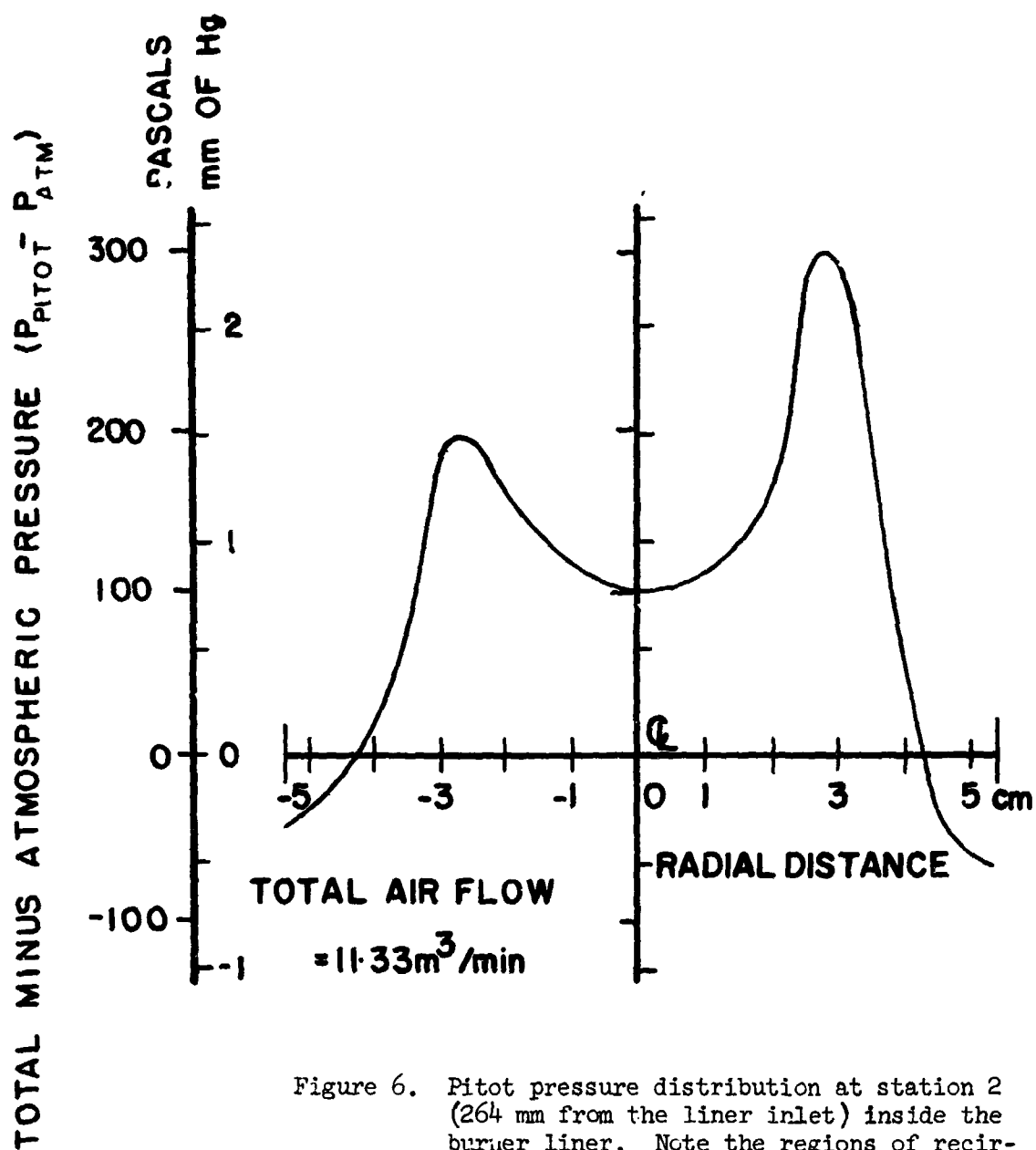
Figure 6. Pitot pressure distribution at station 2 (264 mm from the liner inlet) inside the burner liner. Note the regions of recirculating flow and the asymmetry of flow.

Figure 7.   Blow-off plot giving the maximum total air
            flow rate at flame out as a function of the
            fuel to total air flow rate ratio; 60 per-
            cent total air flow rate is by pass air;
            JP4 fuel.

Figure 8. Speed of sound and theoretical exit plane exhaust temperature as a function of overall fuel/air ratio inside can assuming 60% bypass flow.

Turbulence Measurements

The combustion process, and therefore the noise generated, depends on the turbulent intensity in the combustor can. The scaling laws for sound power and frequency also are influenced by the 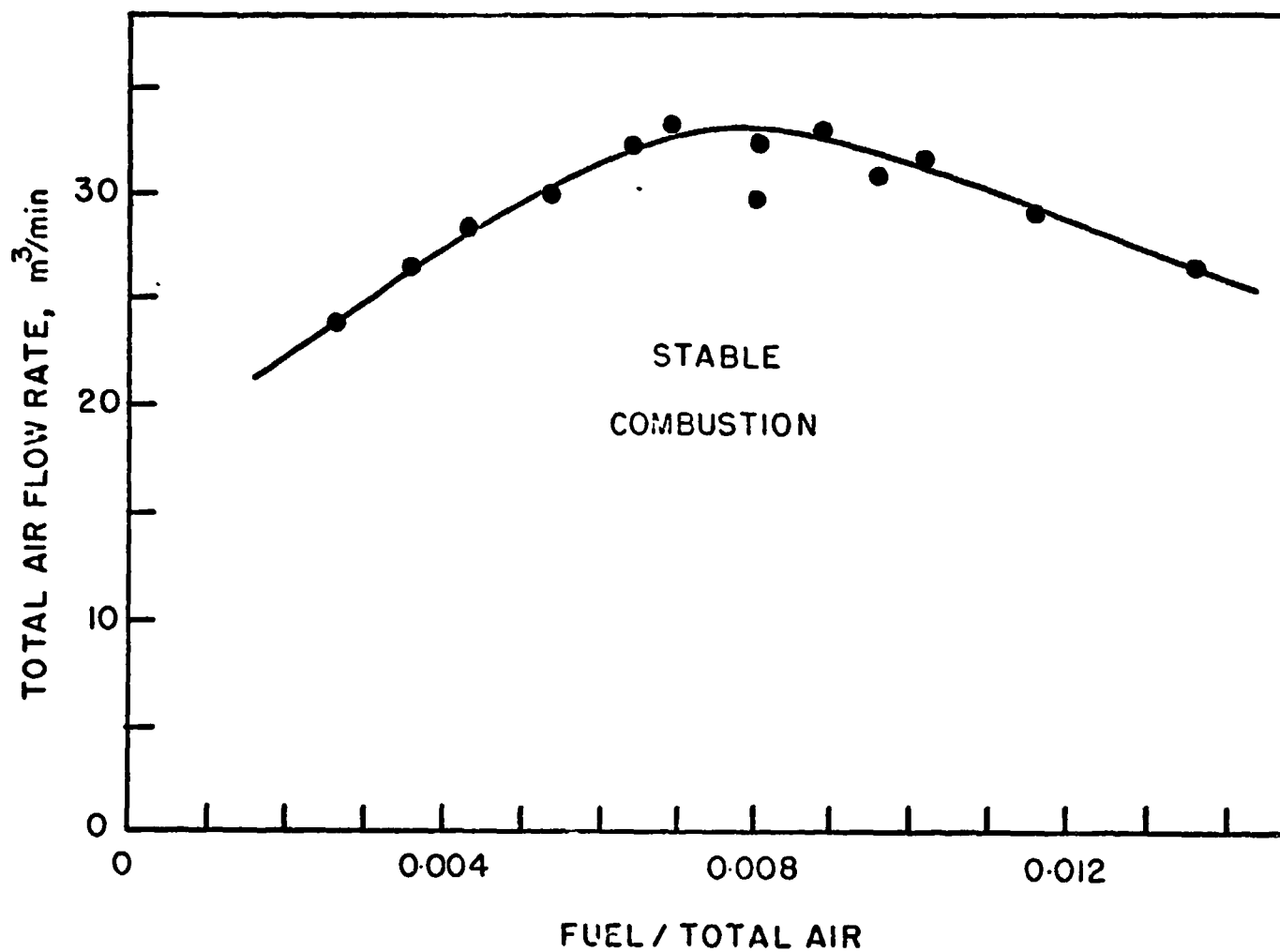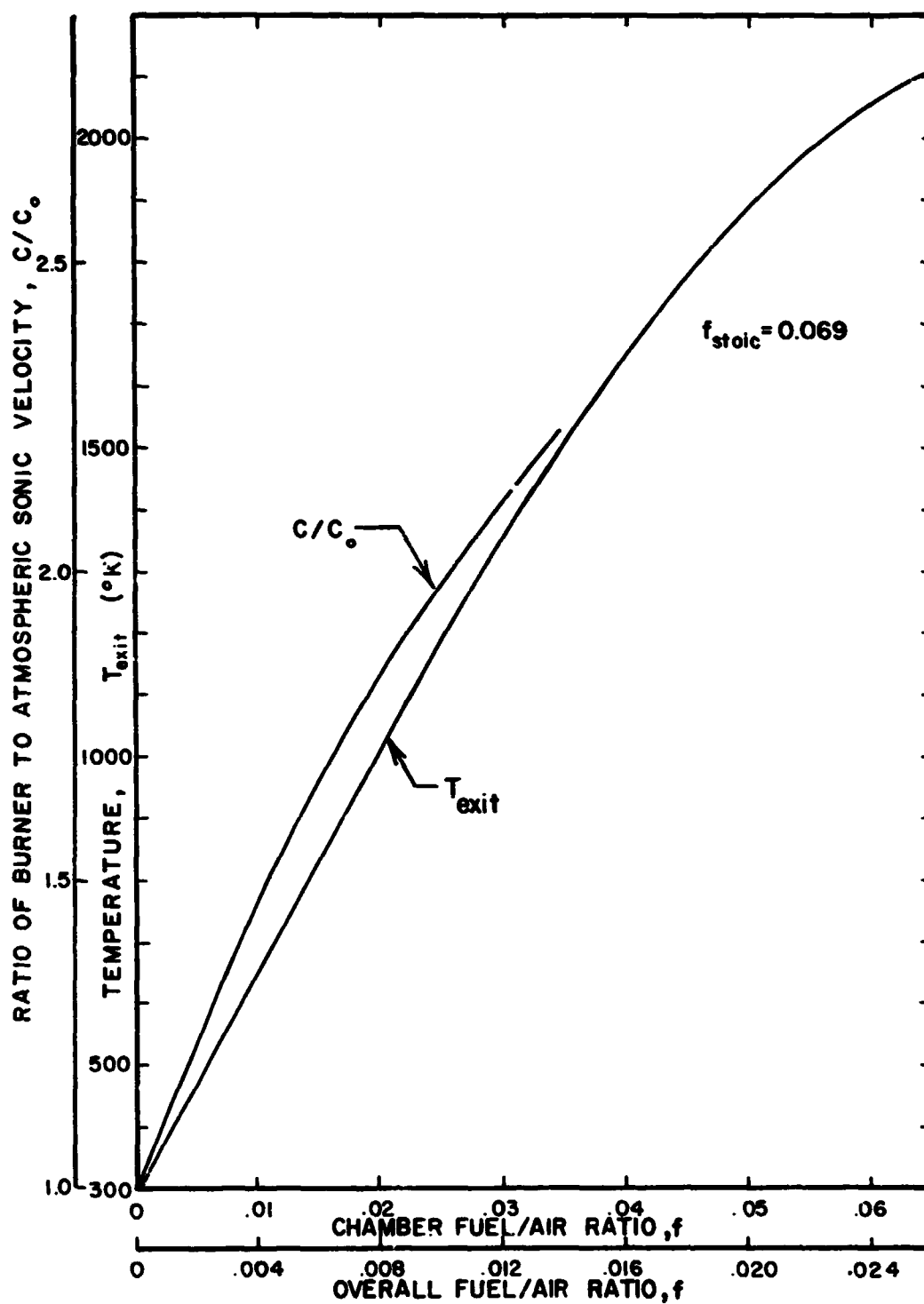scaling of turbulence intensity in the flow. In an attempt to gain some knowledge of the turbulence field that exists in the combustor, hot-wire measurements were made inside the burner liner in cold flow conditions.

A constant temperature single wire (stem was used. The wire was held perpendicular to the flow and was located on the axis of the burner, at 12 cm from the open end. Turbulence intensity was determined at various flow rates of air into the combustor. The data reduction procedure is described in reference 8. The results are presented in Table 1 which shows that intensity of turbulence at the measured location remains almost constant (15-16%) with flow velocity. This result was expected; that is, the relative intensity of turbulence in low subsonic flows is usually independent of velocity.

Table 1. Turbulence Intensity in Combustor (Cold Flow).

Total Air Flow rate m^3/min	11.3	14.1	16.9	19.8	22.6	25.4	28.2
Intensity of Turbulence, %	16	15	15	15	15	16	16

However, it is also true that for fixed configurations the spectra should shift to higher frequencies as the flow velocity increases in accordance with a Strouhal number scaling law. To check this, on line Fourier analysis was conducted of the hot wire signal. The results are shown in Figure 9. The surprising result is that the spectral falloff occurs in the same frequency vicinity, regardless of the flow rate. The spectral shape is independent of the flow velocity. This will aid in later data analysis of the noise results since a connection has previously been noted between the frequency content of combustion noise and the cold flow turbulence spectrum (ref. 9).

Noise Measurements

Microphones for sound pressure measurement were placed at a radius of 3.05 m. This radius was selected based on measurement of sound pressure along the $\theta = 90^\circ$ line which showed that at this radius far field conditions would be satisfied.

The radiated sound powers were calculated from measured sound pressure levels by integration over a spherical surface assuming axial symmetry. For values of sound pressures beyond the last microphone location a value equal to that at the last microphone location was assumed. The validity of such a procedure is established in reference 1.

The repeatability of the experiments has been found to be excellent. The same run on different days reproduces the sound pressure level readings within ± 1 db and the spectra are indistinguishable.
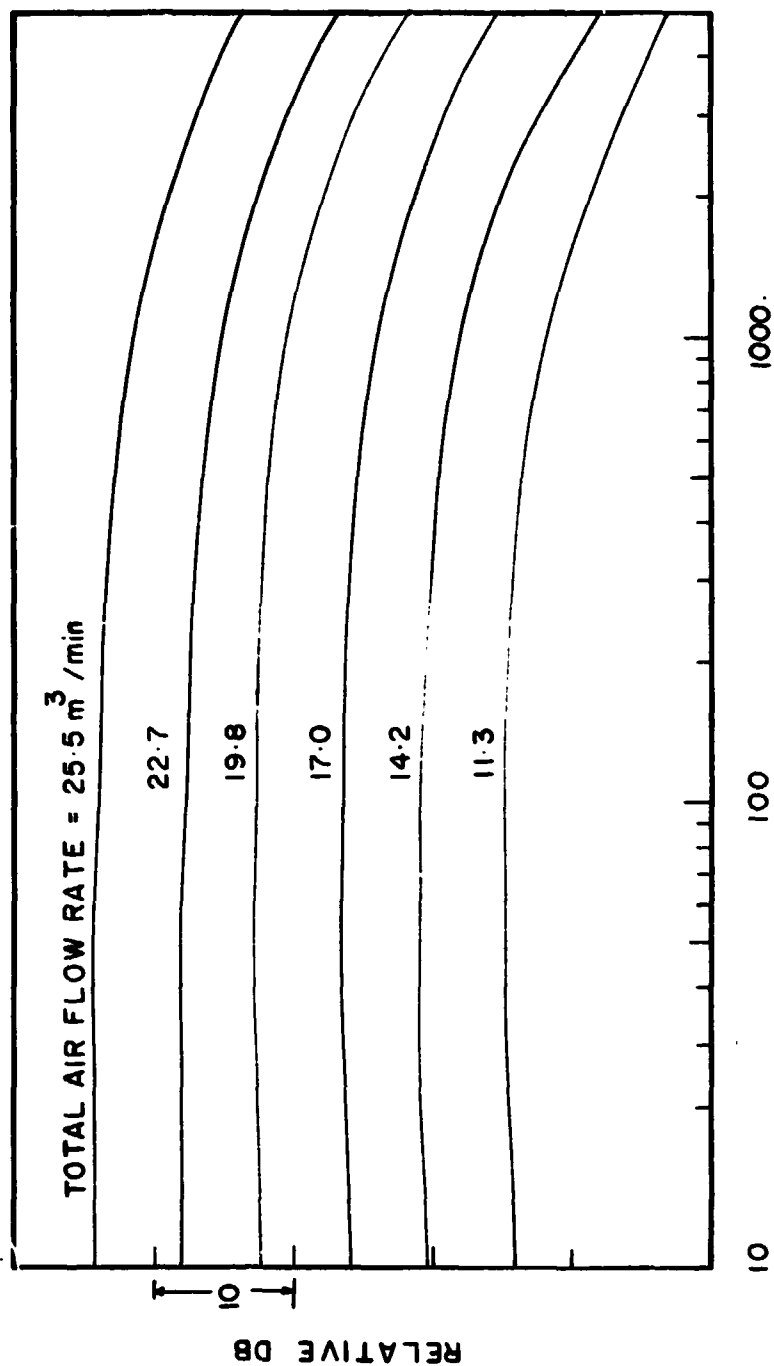
Figure 9. Narrow band spectra of the cold flow turbulence inside the can on the burner axis at 12 cm from the open end; the curves are shifted vertically for clarity and only the curve shape is quantitative.

Ground reflections are present in the experimental noise data presented since the tests are somewhat close to a ground reflecting plane (see figure 3). The microphones at angular locations of 90° and 120° were found to be the closest to the ground surface and hence would have the greatest influence of ground reflections. To determine the extent of dependence of the results on ground reflection, an experiment was conducted in which sound pressure were measured at the 90° and 120° microphones with and without covering the ground between the source and the microphones with fiberglass mats. The mat thickness was at least 50 cm everywhere and this matting is the same as used in the anechoic chamber of reference 1 where it was shown to be quite effective in the frequency range between 125 and 5000 Hz.

The overall sound pressure levels with and without fiberglass covering agreed within 1.1 db, thus showing that the effect of ground reflection upon overall SPL was within reasonable limits. Figure 10 presents the spectra with and without fiberglass covering. Since the spectra were in so close agreement they have been shifted for clarity. In this case the spectra presented are actual X-Y plots as obtained from the Fourier analyzer. It can be seen that the major characteristics of the spectra are unaffected by ground reflections. There is, of course, some effect on the various peaks and lows in the X-Y plot. Most noticeable is the trough at about 210 Hz in the 90° location due to ground reflection which shifts when the fiberglass covering is used. It was therefore concluded from this experiment that the ground reflection effects were small enough to not line the ground with fiberglass when conducting noise measurements.

THEORY

Theoretical considerations applied to the combustion process of the configuration are complicated by the enclosure(can) surrounding the flame; if the flame were open the treatment of reference 9 would be applicable with only slight modification. Furthermore, the gas turbine combustor is technically a diffusion flame, wherein the fuel and oxidizer initially enter the combustor unmixed, and most theoretical success to date has been with premixed flames (ref. 10). As is detailed in Appendix A this configuration represents a transition case whereby neither the treatment of a plane wave duct theory or an open flame theory is strictly valid, but there are the only treatments which are mathematically tractable, within the scope of this program. A previous treatment of this configuration by plane wave duct acoustics has appeared in the literature (ref. 11), but the results were unsatisfactory; the problem stems primarily from the fact that duct acoustics demands strong resonances to be transmitted in the radiated sound which simply do not appear experimentally. One way to have made plane wave duct acoustics valid would have been to place a cylindrical extension on the can in order to sufficiently remove the combustion process from the end plane. However, severe questions would have arisen in the data reduction concerning heat transfer to the extension tube and mixing of the bypass air and combustion gases. Furthermore, combustion instability may have become a problem. Consequently, the noise data has been analysed as though the flame were an open, non-ducted flame in Appendix A. The justification for this analysis is also located in Appendix A.

Using the empirical results that the cold flow turbulence spectra shapes are invariant with flow velocity, as are the combustion noise spectra (as will be seen later), the theory of Appendix A predicts the sound power to scale as

$$P \propto \frac{\rho_o}{4\pi c_o} \ S_{can} \ F^{2a} \ U^4 \ (\frac{H}{c_p T_o})^2 \tag{1}$$
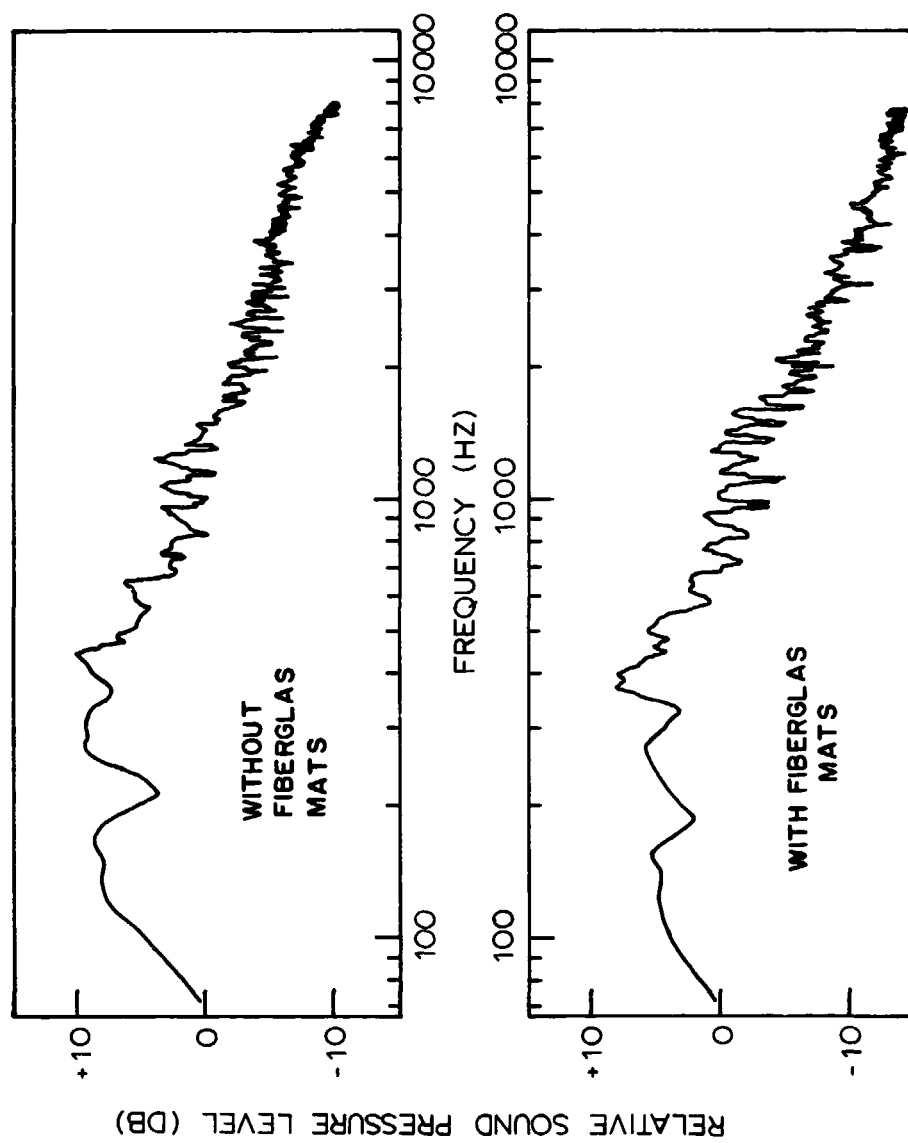
15

Figure 10. Ground reflection effects; comparison of spectra with and without ground acoustic treatment; total air flow rate, 19.8 m³/min; fuel to total air flow rate, 19.8 m³/min; fuel to total air ratio, 0.0085; 60 percent of total air flow is by-pass flow; microphone at 90° off downstream axis.

16

In Eq. (1) there is some theoretical uncertainty concerning the exponent on F because of an uncertainty as to whether the actual F should be used or the stoichiometric value, which is a fixed number. The exponent 'a' should lie between 0 and 2 but the actual value should be experimentally determined. The frequency of maximum radiated power should scale like

$$\omega_c \propto \frac{U}{h\ Re} \tag{2}$$

These formulas will later be compared with the experimental results.

Equation (1) is based upon sound radiation to surroundings with properties denoted by the subscript o. In an actual engine installation the combustor is usually followed by a set of nozzles leading to the first turbine stage and these nozzles usually operate near a choked condition. Consequently, the sound radiation picture is totally different, as compared with radiation to open surroundings. The physical picture which leads to Eq. (1) is a velocity fluctuation downstream of the combustion zone induced by different fluid elements being heated different amounts as they pass through the flame. Consequently, not only is there a velocity fluctuation but there is a temperature fluctuation. Both of these fluctuation types will cause sound waves to be generated when the flow traverses the turbine inlet nozzles. In fact, entropy noise is precisely the noise generated by the hot spots (which are also associated with the velocity fluctuations which cause direct combustion noise). Because the waves generated in the nozzle will propagate both upstream and downstream one must solve the entire can acoustics problem to determine the total amount of sound which gets through the nozzle. The acoustical properties of the can will therefore heavily determine the sound power output and also the emitted spectra. This complete problem has not been solved here.

It seems reasonable, however, as a first approximation that the amount of direct combustion noise which gets out should be proportional to the free flame source strength, and this is the quantity which appears in Eq. (1). The quantity ρ_o/c_o which appears in Eq. (1) is related to the properties of the medium to which the sound is radiating. In the case of an installed configuration the sound is radiating to a fluid which has the properties in the engine. As a first approximation, therefore, for the installed configuration, set ρ_o/c_o to be ρ_1/c_1. Then the scaling law derived from Eq. (1) for installed configurations put in terms of engine variables like pressure, combustor inlet temperature and combustor outlet temperature is

$$P \propto \frac{P}{T_1^{\frac{1}{2}}} \quad S_{can} \quad F^{2a}\ U^4 \left(\frac{H}{c_p T_o}\right)^2 \tag{3}$$

The procedure leading to Eq.(3) is intuitively appealing but it must be cautioned that the spectral response of the can may alter the scaling law, since if the frequency content of the noise shifts with the variables in Eq. (3) the can response may alter the ultimate noise output.

DISCUSSION OF RESULTS

Figure 11 shows directionality patterns obtained at various flow velocities through the combustor for JP-4 fuel. The smooth lines in the figure are polynomials in cos θ fitted by a least square technique to the experimental data points (ref.1). The directionality appears to be quite weak. Over the entire sector of measurement (0-120°) the maximum change in sound pressure level is no greater than 4-5db. Figure 12 shows the directionality pattern at various mixture ratios. The directionality being weak was required for the data reduction procedure used for sound power.
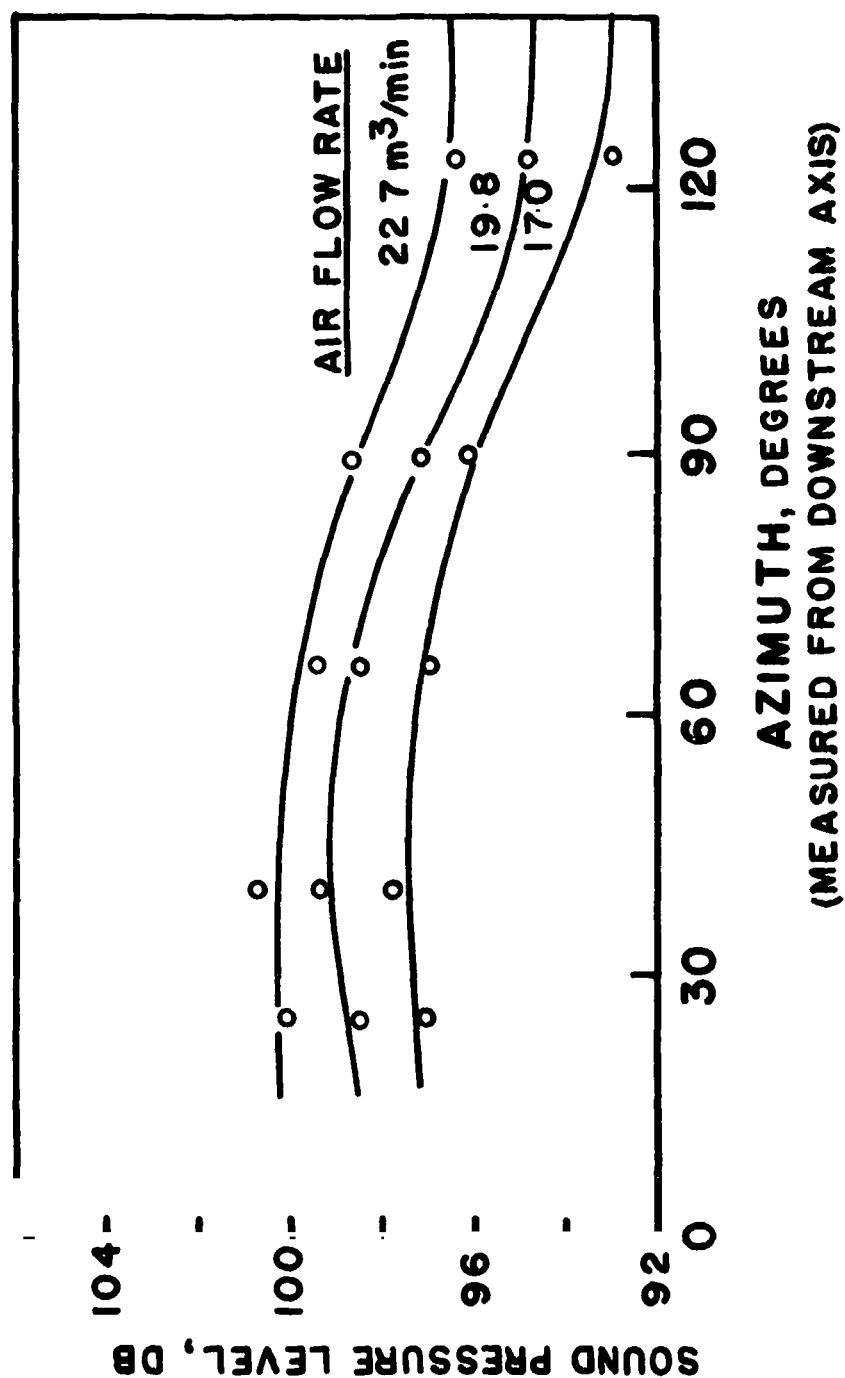
Figure 11. Directionality at various total air flow rates; 60 percent of total air flow rate is by-pass flow; microphone circle radius is 3.05 m; fuel to total air flow rate ratio is 0.009; JP-4 fuel.
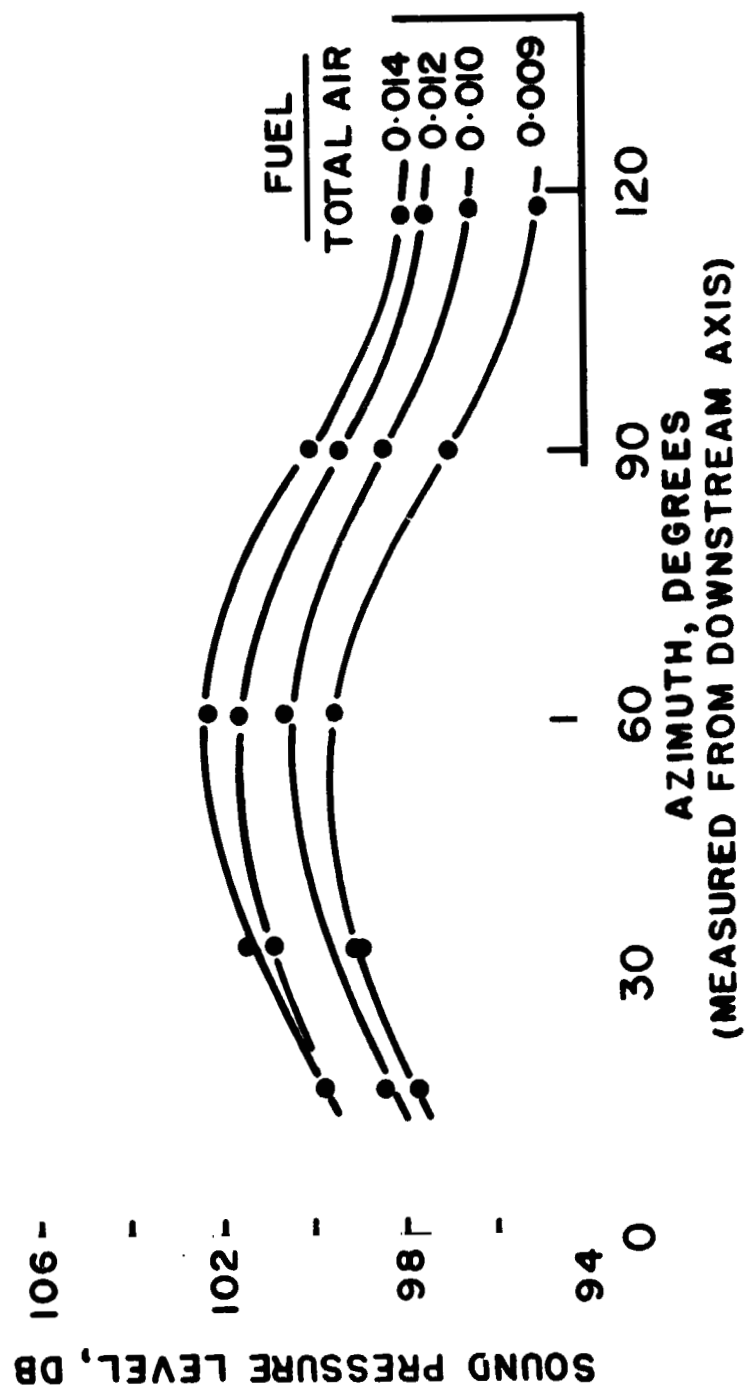
18

Figure 12. Directionality at various mixture ratios; total air flow rate of 19.8 m3/min; 60 percent total air flow rate is by-pass flow; microphone circle radius is 3.05 m.; JP-4 fuel.

In an actual engine configuration this directionality may be altered.

Figure 13 shows the variation of radiated sound power with varying total air flow rates for JP-4 fuel. Sound power is seen to scale with the total air flow rate to an exponent between 2.3 and 2.7. The effect of changing fuel flow at a constant value of total air flow rate is illustrated in figure 14. Figure 14 also shows the behavior of thermoacoustic efficiency (the ratio of radiated sound power to the total thermal input) with varying fuel flow rate and this figure contains results for methanol and acetone. Sound power is seen to be insensitive to fuel flow rate over a wide range of fuel flow rates, except for methanol, which will be discussed below. However, when the mixture ratio increased above approximately 0.008 for JP-4 the sound pressure starts increasing rapidly with fuel flow rate. It is observed that this transition mixture ratio also corresponds to the mixture ratio at which the maximum occurs in the blow-off curve in figure 7. A thermoacoustic efficiency as high as 3×10^{-5} is seen for the noise generated in figure 14. This is the highest known value of thermoacoustic efficiency ever reported for hydrocarbon-air flames.

It was difficult to keep a stable flame with methyl alcohol as the fuel, so there are only two data points reported at which a well-stabilized flame existed for the flow rate of 14.2 m^3/min. Both points for methanol show that acoustic power depends upon F. But notice a curious fact that F_{stoic} for JP-4 and F_{stoic} for methyl alcohol have the ratio F_{stoic}(methanol)/F_{stoic}(JP-4) = 2.3. Consequently, the methyl alcohol results are obtained at an overall F which is roughly the same fraction of the stoichiometric F at which the JP-4 results were becoming sensitive to F. Blowout curves (figure 7) typically maximize at a fuel/air ratio corresponding to a stoichiometric ratio in the primary portion of can type combustors (ref. 12). While a distinct primary zone is difficult to identity for the combustor of this program, because air is taken in the head end as well as through the sides, the JP-4 and methanol results seem to indicate that when the ill-defined primary becomes stoichimetric or fuel rich the noise becomes more heavily dependent on F. On the other hand, viewing the acetone results there is a uniform variation of the noise output with F, but the variation is weak.

The theory of the previous section suggest that the noise power may be expressed in the form $P = K\, U^a\, F^b\, H^c\, S_{L_{max}}^d$ with K,a,b,c and d as constants. The parameter $S_{L_{max}}$ was not included in the theory, but may be added here to see if, there indeed is observed an effect of fuel reactivity, of which $S_{L_{max}}$ is a measure. Taking the logarithm of both sides of the empirical expression, the constant may be determined by a least squares fit to the data. In order to only use data where a unique constant b will fit the data, the JP-4 data for an F above 0.008 have been rejected. However, all the methanol data have been included in order to obtain the fuel type effect, even though the methanol data may be in a regime equivalent to the JP-4 data above an F of 0.008. The result of the least squares analysis is

$$ P \propto U^{2.6}\, S_{L_{max}}^{0.2}\, F^{0.1}\, H^{1.23} \tag{4} $$

where the $S_{L_{max}}$ values, as well as the H values, have been taken from reference 13. The data for the empirical fit include seven acetone runs, four methyl alcohol runs and sixteen JP-4 experiments. The mean error of the fit is 1% and the standard deviation is 16%, well within the accuracy of the measurements. Equation (4) is to be compared with Eq. (1). Theory and experiment agree in the sense that the results are virtually independent of $S_{L_{max}}$, and the fuel type enters mainly through the effect of H. Theory predicts a stronger effect of U than is observed, but both theory and experiment confirm that U is the variable most strongly influencing the noise.
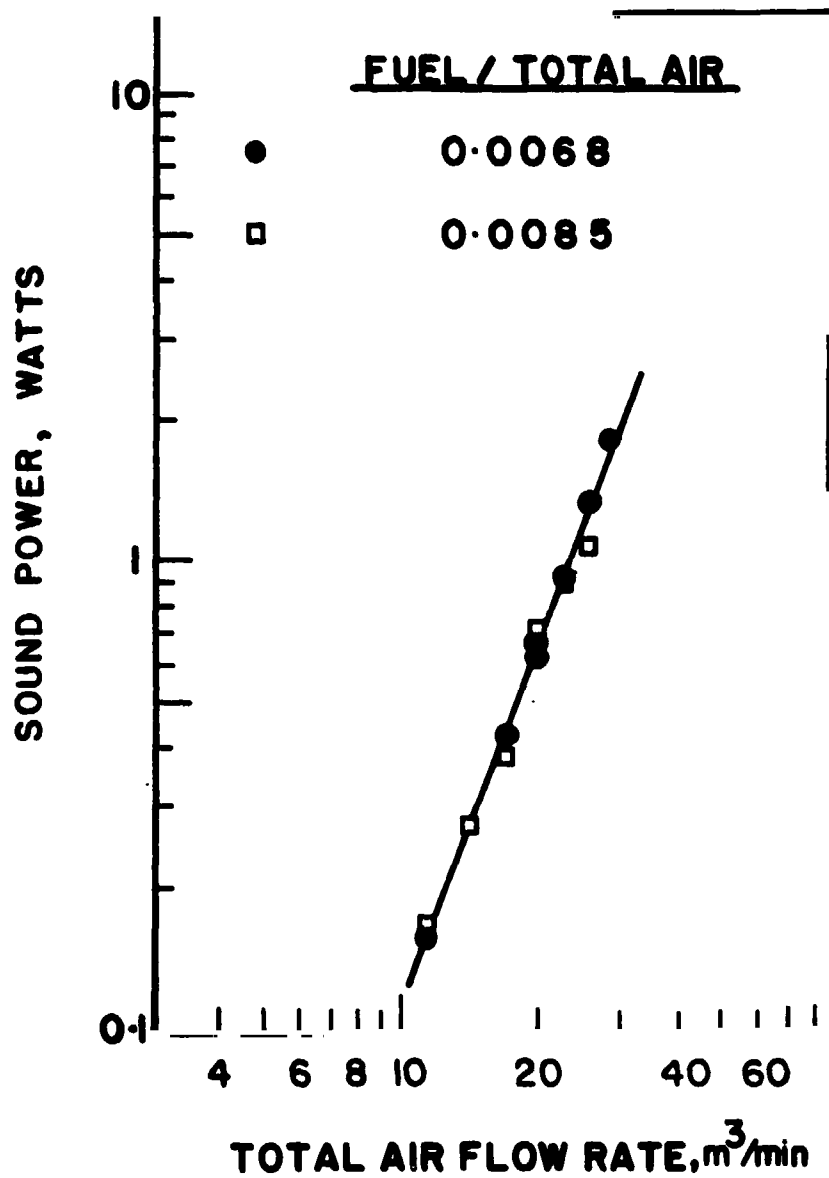
Figure 13. Radiated sound power as a function of total air flow rate; 60 percent of total air flow rate is by-pass flow; JP-4 fuel.
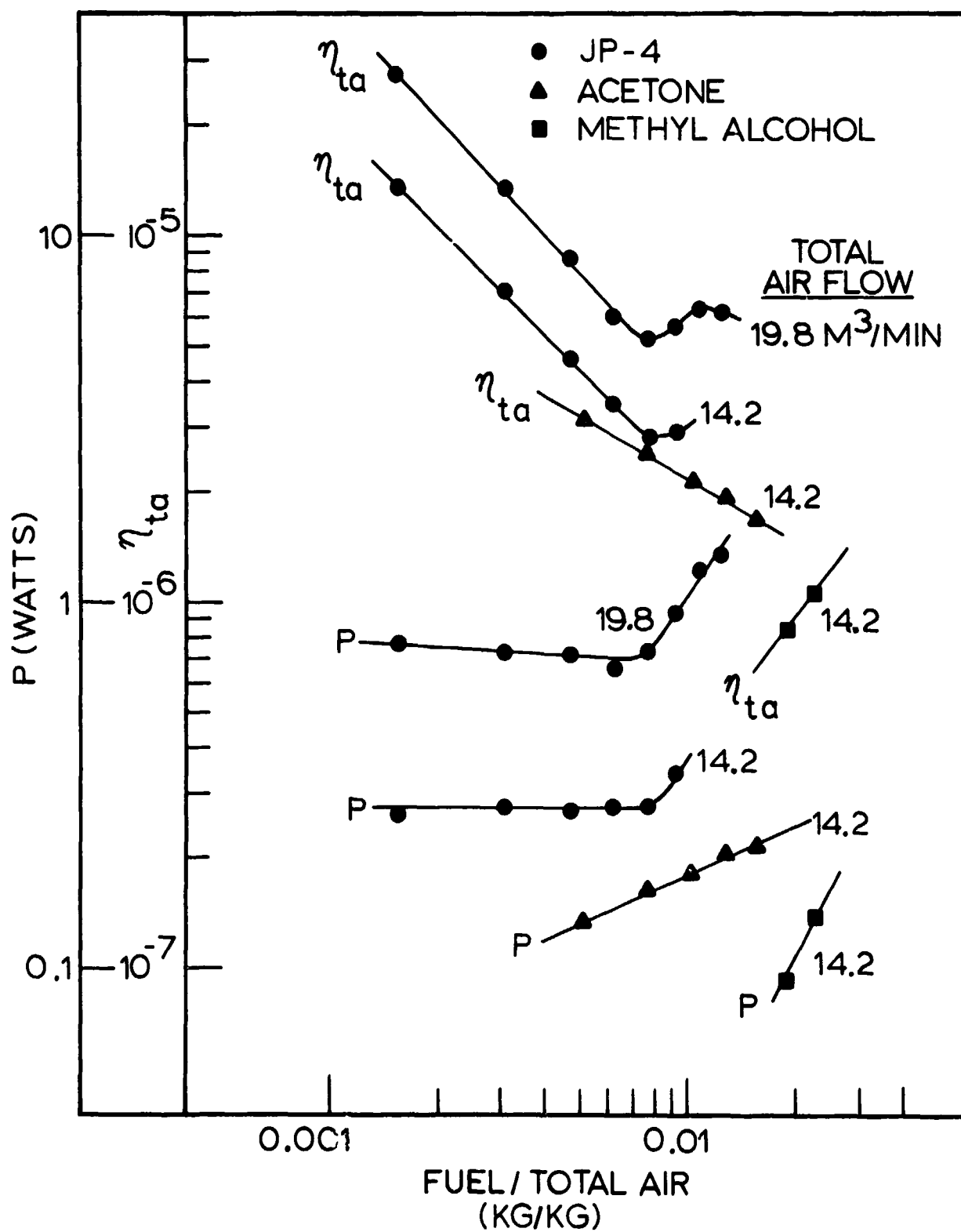
Figure 14. Radiated sound power and thermoacoustic
efficiency as a function of mixture ratio;
60 percent of total air flow is bypass flow.

Figure 15 presents the frequency spectra of noise at both the cold flow (flame off) and flame on conditions. The curves shown are smooth lines drawn through mid-points of the X-Y plot obtained from the Fourier analyzer. It can be seen that combustion noise dominates over the noise due to air flow alone over the entire frequency range. Note, furthermore, the absence of any excited resonances in the air flow spectrum. The combustion spectrum shows that the combustor output is a broad-band noise with a maximum around 400 Hz. Also, weak secondary peaks are seen at frequencies of 1200, 2400, 3600, 4800 Hz etc. Further, almost identical frequency spectra were obtained over the entire sequence of experimental conditions in which the total air flow rates varied from 11.3 to 28.3 m^3/min (at standard temperature and pressure) and mixture ratio (fuel/total air) varied from 0.0014 to 0.02. The spectra taken at various azimuthal locations showed no significant difference in frequency content. This result was extremely surprising, but is a confirmation of the results of reference 9 for a different flame type that the combustion noise spectra are set by the spectra of the incoming cold flow turbulence. It will be recalled that the cold flow can turbulence spectral shapes were invariant with flow rate. The only minor differences seen in the combustion noise spectra were weak shifts in the minor resonances with mixture ratio. Viewing Eq. (2), if the theory and experiment are to agree with one another $\omega_c \propto 1/h^2$ should result. Since the can liner hole size was not varied in this program, this dependence could not be checked. Verification of such a dependence will be part of future efforts.

The 400 Hz spectral peak is not related to a natural mode of the can. If it were, the frequency would shift with mixture ratio (speed of sound). The absence of strong spectral spikes at natural frequencies of the can could possibly be interpreted as an indication the can walls are highly absorbing. This is not believed to be the case because of the work of reference 14; in that work it was shown that walls with a high ratio of solid to open area (as is the case here) with a reasonable flow rate through the holes is a high impedance wall. The interpretation here for the absence of spectral peaks is that the combustion process is a source of primarily velocity oscillations, not pressure fluctuations, within the can. These velocity fluctuations coming out of the tailpipe act as an effective monopole source to the far field. To support this interpretation, pressure measurements should be made inside of the can; this will be done in future work. If the can had been terminated with a nozzle, say, strong spectral peaks could be anticipated because the velocity fluctuations going through the nozzle would require reflected pressure waves. As has been mentioned, this was deliberately avoided in this program. However, in an installed configuration such effects would appear and the acoustical behavior of the entire ductwork would have to be known if the noise output were to be computed.

Consider now a comparison of jet noise with combustion noise. If an acoustic modification factor η_{ac} is defined as the sound power radiated in an installed configuration divided by the sound power radiated by the same flame when burning in the can configuration of this program, it is shown in Appendix B that $\eta_{ta} \eta_{ac}$ F is a unique function of jet velocity for constant values of the jet/combustion noise power ratio. It is known (ref. 15) that if a monopole source is ducted and the walls are hard the source will radiate more power than if it radiated to a free field, due to a change in the radiation impedance of the source. Consequently, η_{ac} can be expected to be greater than unity. Consider a lower limit of η_{ac} =1. Taking η_{ta} = 5 x 10^{-6} as representative of the free flame can-type combustion process, and assuming F= 0.03, F $\eta_{ta} \eta_{ac} \geq$ 1.5 x 10^{-7}. Using the jet noise data of reference 16, figure 16 is constructed.
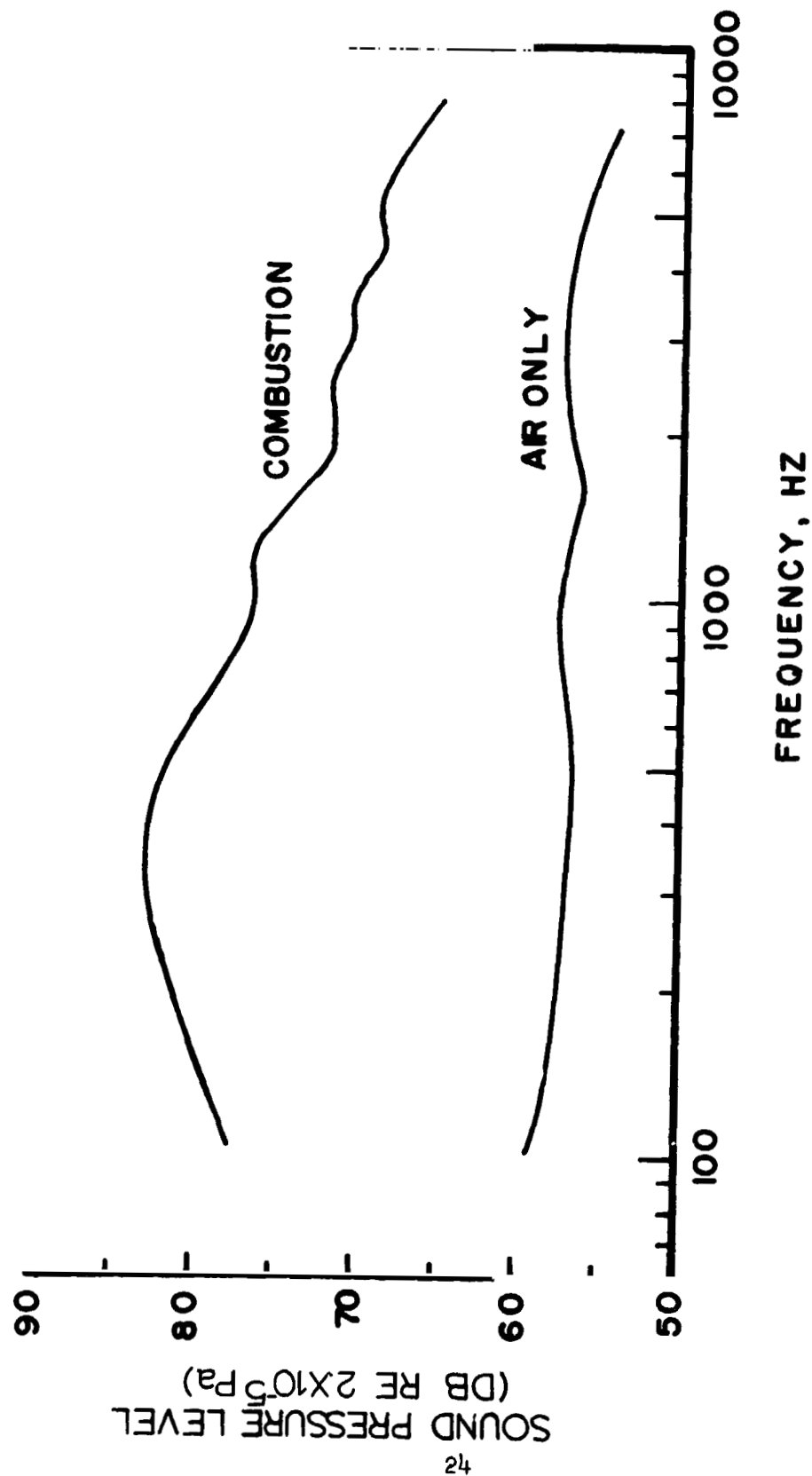
Figure 15. Narrow band frequency spectra of combustion noise and that due to air flow only; band-width is 15.6 Hz; the total air flow rate is 17 m3/min.; the by-pass ratio is 60 percent; the overall fuel to air ratio is 0.0068; the microphone is at the 90° location and 3.5 m from the can exit.
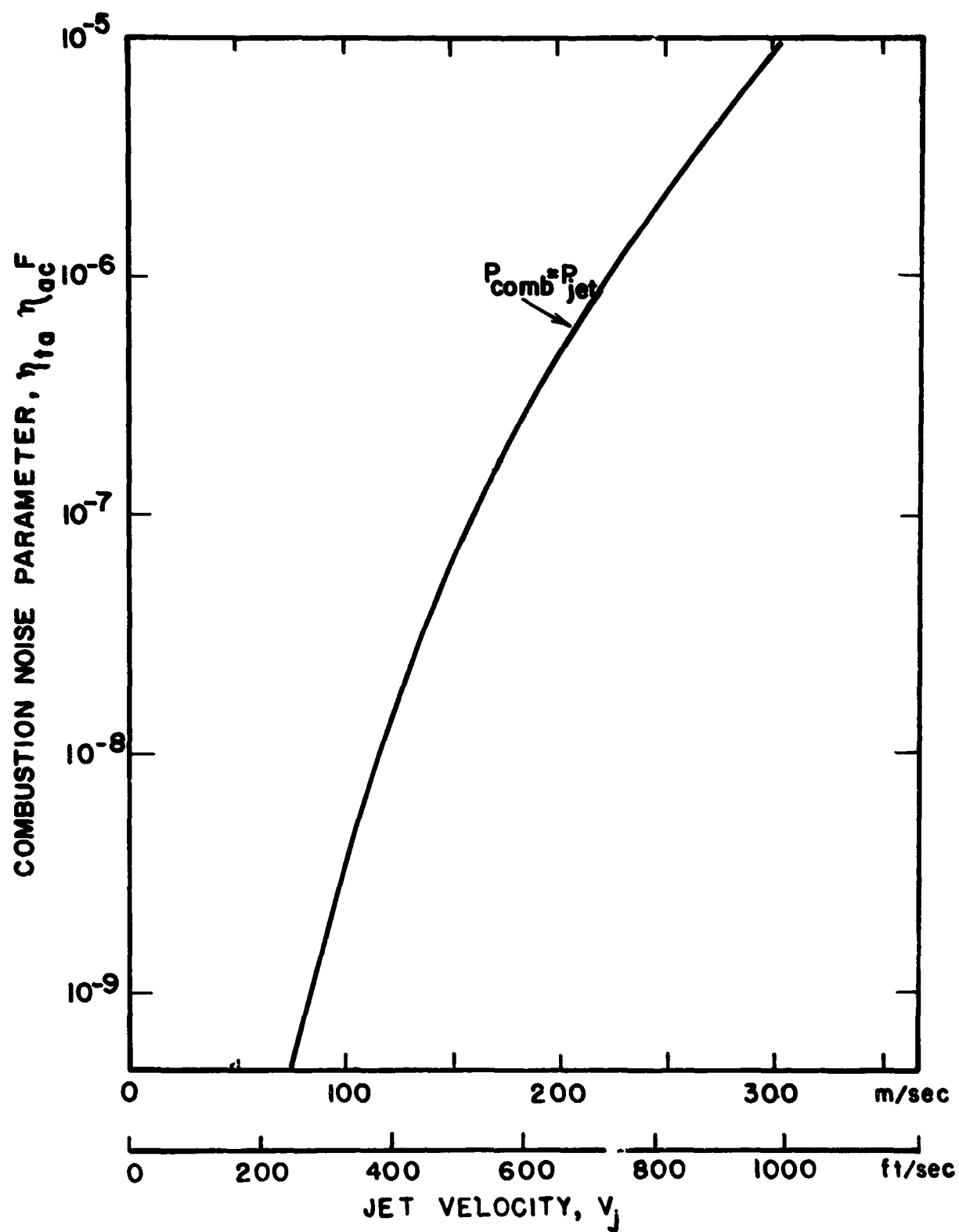
Figure 16. Relative importance of combustion noise to jet noise; no attenuation is assumed as the combustion noise propagates through the engine.

Shown is a line on which combustion noise is equal to jet noise, assuming the η_{ac} value contains no attenuation of the sound power in travelling from the combustor to the engine exit. It is seen from the stated numbers that combustion noise becomes equal to or greater than jet noise above a jet velocity of about 150 m/s.

CONCLUSIONS AND RECOMMENDATIONS

It is concluded that

1. For cans of the general type used in this program and with JP-4 fuel the thermoacoustic efficiency for noise radiation lies in the range 2×10^{-6} to 3×10^{-5}. In an installed configuration the thermoacoustic efficiency is likely to be higher than this value, neglecting any attenuation downstream of the can. However, calculations of the duct effects require accurate knowledge of the duct acoustic properties.

2. The acoustic power radiated is proportional to the effective air flow velocity to an exponent of 2.6. Theroretically the exponent is equal to 4.

3. The acoustic power radiated is only weakly dependent upon fuel/air ratio at low values of this ratio but appears to make a transition to a stronger increase in noise power with fuel/air ratio at some critical fuel/air ratio.

4. In an installed configuration the combustion noise should theoretically be proportional to the pressure, inversely proportional to the square root of the turbine inlet temperature and inversely proportional to the square of the combustor inlet temperature.

5. The primary effect of fuel type on the noise power radiated is through the heat of combustion and not the fuel reactivity. The dependence of sound power output on heat of combustion is one of $P \propto H^{1.2}$. Theoretically, the exponent is 2.

6. There is an invariance of the cold flow turbulence spectral shape with a change in flow velocity and an invariance in the combustion noise spectral shape with a change in all parameters tested. It is a postulate of the theory, which has been verified for other flame types, that the turbulence and combustor noise spectra are linked; the flow variables that will change one will change the other. The observed invariance in spectral shape is a confirmation of the postulate.

7. In can type combustors in installed configurations combustion noise should be at least as large as jet noise for jet velocities below 150 m/s.

As a result of this program it is recommended that

1. Experiments should be conducted varying the liner hole size in order to confirm or reject the theory developed here.

2. Experiments should be conducted with terminating nozzles on the can to determine whether entropy noise or direct combustion noise is the more important noise source.

3. Pressure instrumentation should be employed inside the can to provide confidence in the theoretical model, provide crosscorrelations with the far field pressure and to determine the pressure buildup by can resonances when terminating nozzles are used.

SYMBOLS

a	exponent defined in Eq. (1)
c	speed of sound
c_p	specific heat at constant pressure
f	fuel mass fraction
h	average liner hole size, such as the hydraulic diameter
H	fuel heating value
$\dot{m}$	air mass flow rate
$\dot{m}_f$	fuel flow rate
n	normal
P	sound power
r_o	coordinate vector
Re	Reynolds number based on U and h
S_{cor}	area on the can exit area of close correlation of fluctuating quantities
S_{can}	exit plane area
T	temperature
t	time
u'	velocity fluctuation magnitude normal to the downstream flame surface
u_{rms}	root mean square turbulence velocity of cold flow
U	effective airflow velocity, $\dot{m}/\rho_o S_{can}$
η_{ta}	thermoacoustic efficiency, $P/\dot{m}_f H$

η_{ac} acoustic modification factor

ν frequency

ρ gas density

ω circular frequency

Subscripts

c   frequency at which the maximum occurs in the SPL spectrum

o   cold upstream conditions

1   hot downstream conditions

STOIC   stoichiometric value

$\rightarrow$ vector quantity

REFERENCES

1. Shivashankara, B. N., Strahle, W. C. and Handley, J. C., "Combustion Noise Radiation by Open Turbulent Flames," Aeroacoustics: Jet and Combustion Noise; Duct Acoustics, ed. H. Nagamatsu, AIAA, New York, p. 277, 1975.

2. Shivashankara, B. N., Strahle, W. C., Handley, J. C. and Muthukrishnan, M., "Combustion Generated Noise," Proceedings of the Second Inter-agency Symposium on University Research in Transportation Noise, Vol. II, p. 708, 1974.

3. Abdelhamid, A. N., Harrje, D. T., Plett, E. G., and Summerfield, M., "Noise Characteristics of Combustion Augmented High Speed Jets," AIAA Paper No. 73-189, 1973.

4. Kushida, R. and Rupe, J., "Effect on Supersonic Jet Noise of Nozzle Plenum Pressure Fluctuations," AIAA J., 10, p. 946, 1972.

5. Strahle, W. C., "A Review of Combustion Generated Noise," Aero-acoustics: Jet and Combustion Noise; Duct Acoustics, ed. H. Nagamatsu, AIAA, New York, p. 229, 1975.

6. Anon., "Gas Turbine Engine Assembly, Model 502-7D," The Boeing Co., T. D. 3862-54-3, 18 May 1956.

7. Steffensen, R. J., Agnew, J. T. and Olsen, R. A., "Tables for Adiabatic Gas Temperature and Equilibrium Composition of Six Hydrocarbons," Purdue University Engineering Extension Series No. 122, 1966.

8. Anon., "Hot Wire Measurement of Air Velocity Direction and Temper-ature," Technical Memo Bulletin 94B, Flow Corporation, Watertown, Mass., December, 1964.

9. Strahle, W. C. and Shivashankara, B. N., "A Rational Correlation of Combustion Noise Results From Open Turbulent Flames," Fifteenth Symposium (International) on Combustion, The Combustion Institute, Pittsburgh, Pa., p. 1379, 1975.

10. Strahle, W. C., "The Convergence of Theory and Experiment in Combustion Generated Noise," AIAA Paper No. 75-522, 1975.

11. Strahle, W. C. and Shivashankara, B. N., "Combustion Generated Noise in Gas Turbine Combustors," ASME Paper No. 75-GT-27, 1975.

12. Swithenbank, J., Poll, I., Vincent, M. W. and Wright, D. D., "Combustion Design Fundamentals," _Fourteenth Symposium (International) on Combustion_, The Combustion Institute, Pittsburgh, p. 627, 1973.

13. Anon., "Basic Considerations in the Combustion of Hydrocarbon Fuels with Air," NACA Report No. 1300, p. 451, 1957.

14. Janardan, B. A., Daniel, B. R. and Zinn, B T., "Characteristics of Response Factors of Coaxial Gaseous Rocket Injectors," NASA CR-134788, 1975.

15. Morse, P. M. and Ingard, K. U., _Theoretical Acoustics_, McGraw-Hill, New York, pp. 500-503, 1968.

16. Akuja, K. K., "Correlation and Prediction of Jet Noise," _J. Sound Vib._, _29_, p. 155, 1973.

17. Strahle, W. C., "Some Results in Combustion Generated Noise," _J. Sound Vib._, _23_, p. 113, 1972.

18. Strahle, W. C. and Shivashankara, B. N., "Wall Reflection Effects in Combustion Generated Noise," AIAA Paper No. 75-127, 1975.

APPENDIX A

THEORY OF COMBUSTOR CAN NOISE

In references 9 and 10 a consistent picture of noise production by open flames anchored on the end of burner tubes emerged if it was assumed that a) the cold flow turbulence scaling laws determined the scaling laws for the combustion noise spectra and b) the character of the noise sources was an effective monopole source caused by velocity fluctuations downstream of the flame, not by pressure fluctuations. The velocity fluctuations are caused by different fluid elements being heated differently because of random turbulent excursions in the amount of product gas entrained in a reacting element at the time of reaction. In reference 17 the equivalence of the velocity fluctuations downstream of the flame and the volume distribution of heating rate fluctuations was proven. Therefore, combustion noise may be viewed either as caused by a surface on which there are velocity fluctuations or as a volume containing randomly reacting pocket of gas. One could attempt to extend these concepts to the combustor can situation. A severe complication arises at the outset, however, and that is the effect of the ducting upon the noise radiated.

If the flame were located in a duct, the velocity fluctuations induced by the flame would induce pressure waves radiated as sound which interact with the walls, inducing a back reaction on the flame which changes its radiation impedance. The amount of sound power generated is usually greater than if the flame is not enclosed (refs. 15 and 18) because of the change in radiation impedance. If the duct is long, far enough from the source pure plane waves develop, if the frequencies are below those of the first transverse mode of the duct. If the duct is open to the atmosphere there will be reflections of the incident waves caused by the impedance mismatch between the tube and the open end. A stationary noise standing wave system would then be set up in the tube and this should be calculable as a plane wave problem according to the results of reference 18.

In the present experiments the frequency content of the noise certainly qualifies it for a plane wave problem since the first transverse mode would not occur for this can until $\nu = 3500$ Hz for $c = 600$ m/s. The problem is that the duct is not long enough for purely plane waves to be set up. In fact, there are no strong resonances, at frequencies corresponding to longitudinal modes of the can, ever seen in the data. The open end of the can is not behaving as an impedance mismatch plane to cause reflected waves back into the can. This situation may be interpreted as one of velocity fluctuations at the tailpipe with negligible pressure fluctuations. The radiating surface is the tail-

32

pipe open area and now the problem resembles that of an open flame radiating to free surroundings. To be sure, if an extension were placed on the can that were long enough, duct modes would be seen. This was not done in this experiment because of heat transfer problems and the requirement in the data reduction for taking into account temperature gradients.

Another possible interpretation of the experimental results is that the can walls are highly absorbent to sound so that the only thing left to radiate sound is the presence of velocity fluctuations at the tailpipe. It is not believed that this is the case, however, because of the work of reference 14; the can walls should be acoustically hard.

Given the velocity fluctuations at the exit plane as the acoustic source, the problem may be analyzed exactly as in reference 9, neglecting scattering by the external can surfaces. The result for the acoustic power radiated is

$$P = \frac{\rho_o}{4\pi c_o} < \left[\int_{S_{can}} \frac{\partial u'}{\partial t} \cdot \underset{\sim}{n}_o \, dS(r_o) \right]^2 > \qquad (A-1)$$

The order of magnitude of Eq. (A-1), estimated in the same manner as in reference 17, is

$$P \text{ is } O \left[\frac{\rho_o}{4\pi c_o} S_{cor} \, S_{can} \, u'^2 \, \omega_c^2 \right] \qquad (A-2)$$

Using the postulate that the frequency should scale as the "frequency" of the energy containing eddies of the incoming turbulence, as measured in cold flow,

$$\omega_c \propto \frac{u_{rms}}{S_{cor}^{\frac{1}{2}}} \qquad (A-3)$$

Experimentally it was found that $u_{rms} \propto U$ but that ω_c was independent of U. From dimensional analysis $S_{cor}^{\frac{1}{2}} \propto h \, f(Re, M, F)$ is to be expected. For low Mach number flows, however, Mach number usually disappears as a relevant dimensionless group and only Re and F should remain relevant. Experimentally, however, ω_c was found independent of F. The only way that ω_c can be independent of U, therefore, is for the following scaling law to hold:

$$\omega_c \propto \frac{U}{S_{cor}^{\frac{1}{2}}} \qquad (A-4)$$

33

$$S_{cor}^{\frac{1}{2}} \propto h\ Re \qquad\qquad (A-4)$$

Eqs. (A-3) and (A-4) have the interesting consequence that as the liner hole size is changed the frequency spectra should change. This effect was not investigated in this program.

Now u' is interpreted as the sound causing impetus which in turn is caused by the combustion process. In reference 9 it was found that u' could be taken to be proportional to the velocity change in going from unburned to burned gases. For a constant pressure, constant area heating process

$$\rho_o U = \rho_1 U_1$$

$$\rho_o/\rho_1 = T_1/T_o = \left(1 + \frac{FH}{c_p T_o} \right)$$

Then for $u' \propto U_1$,

$$u' \propto \left(1 + \frac{FH}{c_p T_o} \right) U \qquad\qquad (A-5)$$

The work of reference 9 was based on premixed flames. The flame here is a diffusion flame wherein the air and fuel enter the combustion chamber in an unmixed state. This causes some ambiguity in the interpretation of F in Eq. (A-5). That is, the concern here is with fluctuations, and fluctuations in F will occur. In fact, some elements may burn with $F = F_{STOIC}$ while other elements can burn either fuel lean or fuel rich. It might appear reasonable to choose $F = F_{STOIC}$ in Eq. (A-5) to measure the maximum fluctuation in u' that might be attainable; on the other hand, surely as F gets lower and lower one would expect the overall magnitude of the heating fluctuation to decrease. To allow for this uncertainty, Eq. (A-5) is replaced by

$$u' \propto F^a \frac{H}{c_p T_o} U \qquad\qquad (A-6)$$

$$0 \leq a \leq 1$$

with the exponent "a" to be determined by experiment. In Eq. (A-6) it has been assumed that $FH/c_p T_o \gg 1$. If $a = 1$, the case of using F instead of F_{STOIC} is under consideration. If $a = 0$ is observed experimentally, an indication is given that $F = F_{STOIC}$ should be chosen in Eq. (A-5).

Placing Eqs. (A-6) and (A-7) into Eq. (A-2), there results

$$P \propto \frac{\rho_o}{4\pi c_o} \, S_{can} \, U^4 \, F^{2a} \, (H/c_p T_o)^2 \qquad \text{(A-7)}$$

as the final theoretical scaling law for acoustic power. This is reproduced as Eq. (1) in the text.

More correctly, to keep the order of magnitude of Eq. (A-5) the same, Eq. (A-6) should better be represented by

$$u' \propto F^a \, F_{STOIC}^{\,1-a} \, \frac{H}{c_p T_o} \, U$$

In this case

$$P \propto F^{2a} \, F_{STOIC}^{\,2(1-a)} \, (H/c_p T_o)^2$$

would result. Since F_{STOIC} is a function of fuel type a modification of Eq. (4) of the text would result. The regression fit including $F_{STOIC}^{\,2(1-a)}$ would modify the exponent on $H/c_p T_o$. The result including this effect is to replace Eq. (4) by

$$P \propto U^{2.6} \, S_{L_{max}}^{\,0.2} \, F^{0.1} \, F_{STOIC}^{\,1.9} \, H^{3.3}$$

APPENDIX B

RELATION BETWEEN JET NOISE AND COMBUSTION NOISE

From the data of reference 18 the overall power radiated by pure jet noise may be put in the form

$$P_{jet} = 2.6 \times 10^6 \frac{C M_j^{9.1} \dot{m}}{\rho_o U_j} \quad \text{Watts} \qquad (B-1)$$

where M_j is the jet Mach number based on the <u>ambient</u> speed of sound, ρ_o is the ambient density and U_j is the jet velocity. In this formula $\dot{m}$, U_j and ρ_o are in units of kg/s, m/s and kg/m^3, respectively. C is a factor accounting for the directionality pattern given by

$$C = \frac{1}{8M_c} (1 - 0.94 M_c)^5 \left[\frac{1}{(1-M_c)^4} - \frac{1}{(1+M_c)^4} \right] \qquad (B-2)$$

where M_c is the convection Mach number equal to $0.65 M_j$. Combustion noise is given by

$$P_{comb} = \dot{m} F H \, \eta_{ta} \, \eta_{ac} \qquad (B-3)$$

Substituting Eq. (B-3) into Eq. (B-1)

$$\eta_{ta} \, \eta_{ac} \, F = \left(\frac{P_{comb}}{P_{jet} \, H} \right) \left(\frac{2.6 \times 10^6 \, C \, M_j^{9.1}}{\rho_o U_j} \right) \qquad (B-4)$$

Choosing sea level conditions and JP-4 fuel, the right hand side of Eq. (B-4) is a unique function of jet velocity for fixed ratios P_{comb}/P_{jet}.

Equation (B-1) is developed from the data of reference 18 by a) using the correlation for overall sound pressure level at 20° off the downstream axis, b) using the analytical law for directionality given in that reference and c) integrating over a far field sphere to obtain the sound power.